Süleyman Demirel Üniversitesi Fen Edebiyat Fakültesi Fen Dergisi
Süleyman Demirel University Faculty of Arts and Sciences Journal of Science
2021, 16(2): 513-522
DOI: 10.29233/sdufeffd.996120
Atıf için / For Citation: A. Pehlivanlı, M. H. Bölükdemir, "The effect of proton and helium ıons on secondary neutron production in the slab head phantom", *Süleyman Demirel Üniversitesi Fen Edebiyat Fakültesi Fen Dergisi*, 16(2), 513-522, 2021.

Research Article

The Effect of Proton and Helium Ions on Secondary Neutron Production in the Slab Head Phantom

Adem PEHLİVANLI[1,2], Mustafa Hicabi BÖLÜKDEMİR[*3]

[1]*Gazi University, Graduate School of Natural & Applied Sciences, Dept.of Physics, 06500, Ankara, Turkey*
[2]*Kirikkale University, Vocational School of Health Services, Dept. of Medical Imaging Techniques, 71450, Kirikkale, Turkey*
[3]*Gazi University, Faculty of Sciences, Physics Department, 06500, Ankara, Turkey*

**corresponding author e-mail: hicabi@gazi.edu.tr*

(Received: 15.09.2021, Accepted: 09.11.2021, Published: 25.11.2021)

Abstract: Particle therapy (PT) usually uses protons and carbon ions. In addition, the use of low-Z ions (such as He, O, Ne) with higher relative biological effects than protons is also being investigated. Although in PT the majority of the dose is delivered to the tumor volume by the primary particle, a negligible additional dose is left due to the contribution of secondary particles produced by the interaction between the therapeutic beam and the patient's tissues. In particular, neutrons can increase the risk of secondary cancer by transferring energy far away from the treated area. To use charged particles in radiation therapy, it is crucial to characterize secondary neutrons produced (SNP) as a result of primary particle interactions with human tissue. The SNP can be detected with the detector or by methods such as Monte Carlo (MC) simulation. In our study, the total number of neutrons produced in the slab head phantom by proton and He ion beams with an energy of 50-100 MeV/u, the doses stored by neutrons and all other particles were calculated with the Particle and Heavy Ion Transport Code System (PHITS) MC code. The number of SNP by He ion beam increased 7-14 times compared to proton beams. It was calculated that the doses of the SNP by protons were between 11.5% - 16.4% of those in the He ion beams.

Key words: Particle therapy, Secondary neutron, Monte Carlo, PHITS

Baş Plaka Fantomunda Proton ve Helyum İyonlarının İkincil Nötron Üretimine Etkisi

Öz: Parçacık tedavisinde (PT) genellikle protonlar ve karbon iyonları kullanılır. Fakat protona göre bağıl biyolojik etkileri daha yüksek olan düşük Z'li iyonların (He, O, Ne gibi) kullanımı da araştırılmaktadır. PT'de dozun büyük kısmı, birincil parçacık tarafından tümör hacmine verilmesine rağmen, terapötik ışın ile hastanın dokuları arasındaki etkileşim tarafından üretilen ikincil parçacıkların katkısı nedeniyle ihmal edilemeyecek miktarda ek doz bırakılır. Özellikle nötronlar, tedavi edilen alandan çok uzağa enerji aktararak ikincil kanser riskini artırabilmektedir. Radyasyon tedavisinde yüklü parçacıkları kullanmak için insan dokusuyla birincil parçacık etkileşimleri sonucunda üretilen ikincil nötronları karakterize etmek çok önemlidir. Üretilen ikincil nötronlar detektör veya Monte Carlo (MC) benzetimi gibi yöntemlerle belirlenebilmektedir. Çalışmamızda 50-100 MeV/u enerjili proton ve He iyon ışınları tarafından baş plaka fantomunda üretilen toplam nötron sayıları, nötronlar ve tüm parçacıklar tarafından depolanan dozlar Particle and Heavy Ion Transport Code System (PHITS) MC kodu ile hesaplanmıştır. He iyon demeti tarafından üretilen ikincil nötron sayısı, proton demetlerine kıyasla 7-14 kat arttı. Protonlar tarafından üretilen ikincil nötron dozlarının He iyon demetlerindeki dozların %11.5 - %16.4'ü arasında olduğu hesaplandı.

Anahtar kelimeler: Parçacık tedavisi, İkincil nötron, Monte Carlo, PHITS

Adem PEHLİVANLI, adempehlivanli@kku.edu.tr, ORCID: https://orcid.org/0000-0003-4696-9311
Mustafa Hicabi BÖLÜKDEMİR, hicabi@gazi.edu.tr, ORCID: https://orcid.org/0000-0002-7911-7863

1. Introduction

Particle therapy (PT) is a technique that uses accelerated ions (such as protons and carbon) to destroy tumors [1]. Protons and ^{12}C ions with energies of several hundred MeV/u are generally used in PT. In addition, the use of low-Z ions (He, O, Ne) to optimize processes using particles with different relative biological effectiveness (RBE) and oxygen evolution rate (OER) is also being investigated [2]. Treatment with charged particles provides better protection of healthy tissues around the target volume. Therefore, PT offers both physical and biological advantages in the eradication of established tumors, as it has better dose distribution at the target volume compared to photon radiotherapy [3]. Proton and carbon ions are widely used in PT clinical practices. Besides, interest in the application of helium and oxygen ions has been increasing recently [4].

PT is known to be advantageous in the treatment of skull base tumors [5]. Between 1977 and 1992, the first clinical experience with especially helium, carbon and neon ions took place at the Lawrence Berkeley Laboratory, with exciting results (especially in skull base tumors and paraspinal tumors) [6]. Regional values for RBE are higher for PT and depend on many factors that must be considered during treatment planning [7]. In PT, the majority of the dose is delivered to the tumor volume by the primary particle. In addition, a non-negligible additional dose is stored in the tumor due to the contribution of charged and neutral secondary particles produced by the interaction between the beam and the patient's tissues. In particular, neutrons can transfer energy far away from the treated area and increase the risk of developing secondary cancer years after undergoing treatment [8]. To use charged particles in radiation therapy, it is crucial to characterize SNP as a result of primary particle interactions with human tissue. The SNP can be detected with the detector or by methods such as Monte Carlo (MC) simulation.

Several MC simulation codes are used in proton therapy facilities to make better dose estimations [9–13]. In proton therapy, GEANT4 and MCNPX MC codes are used to compare energy distributions in phantoms with different properties and geometries [13]. With MC codes such as FLUKA, GATE and PHITS, the most appropriate beam parameters for proton therapy can be determined [11]. The energy distribution of monoenergetic neutrons at different depths in tissue-like phantoms was calculated with the GEANT4 MC code [12]. The relationship between the biological effects of neutrons and their field properties was analyzed with the PHITS MC code [9]. The cross sections of neutron production by protons with 135 and 180 MeV energies were calculated to be used in the calculation of neutron dose and the results were compared with PHITS, FLUKA and GEANT4 MC code [10]. Low-density plastics used for collimation in proton therapy produce fewer neutrons compared to metals, and it has been reported that the deposited dose of secondary neutrons increases when metal density increases [14].

In many studies, the angular and energy distributions of SNP as a result of bombardment of targets of different thicknesses with He ions in a certain energy range have been determined by scintillation detectors [15–20]. By bombarding different targets with He ions in the HIMAC facility, the flux of secondary neutrons at different angles to the forward direction of the ions was calculated and compared with previously published experimental data and the MCNPX MC code [21]. Thermal and total neutron fluxes at Bragg peak energies in 30×30×30 cm^3 phantom with ICRU soft tissue feature were calculated with MCNP MC code [22]. Neutrons produced by different particles such as Proton and He ions in a cylindrical water phantom with a radius of 10 cm and a length of 30 cm were calculated with the SHIELD-HIT MC code [23]. In the above-

mentioned studies, secondary neutron measurements from He ions were investigated, but it is known that experimental data on this subject are limited [24].

Secondary neutron production by therapeutic energy protons in the slab head phantom ranges from 0.27% to 10.14% [25]. In our study, the lowest energy was determined as 50 MeV/u, which will form a Bragg peak right after the cranium, and 100 MeV/u, which will reach the midpoint of the phantom, as the highest energy. The total number of SNP in the slab head phantom for the sent proton and He ions, the contribution of neutrons and other particles to the absorbed dose was calculated by PHITS MC simulation. Thus, the effect of helium ions on secondary neutron production and comparison with that of protons were investigated.

2. Material and Method

2.1 Head Phantom

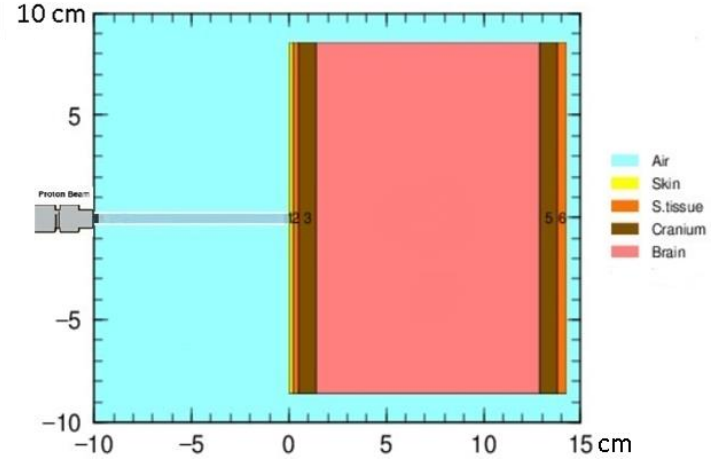

Figure 1. Slab head phantom geometry and pencil beam view taken from PHITS.

Various phantoms are used in radiotherapy for treatment planning of different parts of the human body. Three types of phantoms are suggested for the head or spinal cord: slab, cylindrical and Alderson phantom [26]. Plate phantoms show depth dependent effects more clearly. For this reason, the slab head phantom in Figure 1, which was created to show the cross-section of the head structure, was used in our study. The slab head phantom includes from left to right 0.2 cm of skin, 0.3 cm of soft tissue, 0.9 cm of cranium, 11.5 cm of brain, 0.9 cm of cranium, and finally 0.5 cm of soft tissue. Figure 1 shows that the beam interacts with the air at a distance of 10 cm, and in the head phantom, it reaches the brain by passing through the skin tissue, soft tissue, and cortical bone, respectively. According to the maximum dimensions of the brain used in the MIRD-ORNL phantom, the side dimensions of the phantom were accepted as 17.2 cm × 13.2 cm, as in different studies [25, 27]. In our calculations, the atomic densities and percentages of the tissues are given in Table 1, taking into account the slab head phantom consisting of different layers.

Table 1. Basic compositions and mass density of tissues in the Slab Head phantom (compositions are expressed as percentage by weight) [25]

Tissue Type	Density (g/cm^3)	H	C	N	O	Ca	Na	P	S	Cl	K
Skin	1.09	10	20.4	4.2	64.5	-	0.2	0.1	0.2	0.3	0.1
Soft Tissue	1.03	10.5	25.6	2.7	60.2	-	0.1	0.2	0.3	0.2	0.2
Cranium	1.61	5	21.2	4.0	43.5	17.6	0.1	8.1	0.3	-	-

Brain	1.04	10.7	14.5	2.2	71.2	-	0.2	0.4	0.2	0.3	0.2

2.2 Pencil Beam

Pencil beams with therapeutic energy were sent perpendicular to the tissue sections as in Figure 1. Range modulator wheel, patient-specific aperture and compensator are not required for the pencil beam system beamline in the selected geometry. In this case, secondary particle generation in the beamline is ignored. Therefore, the main source of secondary particles for pencil beam systems is the interaction of primary particles with the patient, not the beam delivery system [28]. In this study, only the interactions of ions with body tissues were considered. Energy choices were determined for two different particles (1.7, 2.5, 3.4, 4.5, 5.6 and 6.9 cm) with the same Bragg peak positions. SNP in the head phantom of ion beams of selected energies (therapeutic energies) was calculated.

2.3 PHITS Physics Model

In this study, MC-based PHITS code is used which can transport particles with energies up to 1 TeV (per nucleon per ion) using several nuclear reaction models and data libraries. The PHITS MC code reveals particle-matter interaction results using various "Tally" prediction functions such as Product-Tally, and Deposit-Tally. T-Deposit tally is the energy loss of the charged particles and nucleus, and the absorbed energy (Gy/particle, MeV/particle); T-Product tally calculates secondary particles (1/particle) produced by nuclear reactions, decays and fission. The deposited energy of neutrons is generally obtained from nuclear data and Kerma factors [29, 30]. PHITS code can simulate nuclear reactions with using theoretical models or and nuclear data libraries. For proton-induced reactions, it uses the INCL-4.6 [31] model by default. For all energy calculations, the error rate was obtained around 0.05% by simulating 10^6 events. This program is extremely flexible as it allows to define inputs such as materials, geometries, targets and particle properties. The calculation results may allow us to have information about the particle to be used in terms of the number of SNP in the PT and the contribution of the dose from the neutrons.

3. Results

3.1 Secondary Neutrons

All non-primary particles originate from primary or secondary particles. Neutrons are the most important secondary particles because they are uncharged. Neutrons can be produced by elastic scattering of neutrons on the target nucleus or by nuclear reactions. The mean free path of fast neutrons in matter is typically much longer compared to the ranges of protons with the same energies, since protons suffer a direct loss of energy due to ionization of target atoms, but neutrons do not. Therefore, the dose associated with neutrons is expected to be dispersed in a much larger volume compared to protons. The secondary neutron dose is related to the number of neutrons released by the interactions. The neutron production was found in water per 100 MeV proton with GEANT4 as 0.040 [32] without any restriction on the neutron initial energy. We obtained 0.051 neutrons per 100 MeV incoming proton with the PHITS MC program. The number of neutrons produced by the PHITS simulation program for proton with 60 - 100 MeV energies in the (50×10×50) cm^3 water phantom is shown in Figure 2.

It is important to compare their effects in these two cases, as secondary neutrons are produced in both proton and heavy ion irradiations. The role of SNP in the interaction of protons with thick targets has been previously investigated in some experimental and

theoretical studies specifically targeting medical applications [33, 34]. There is limited information on doses from secondary neutrons generated in ion irradiations.

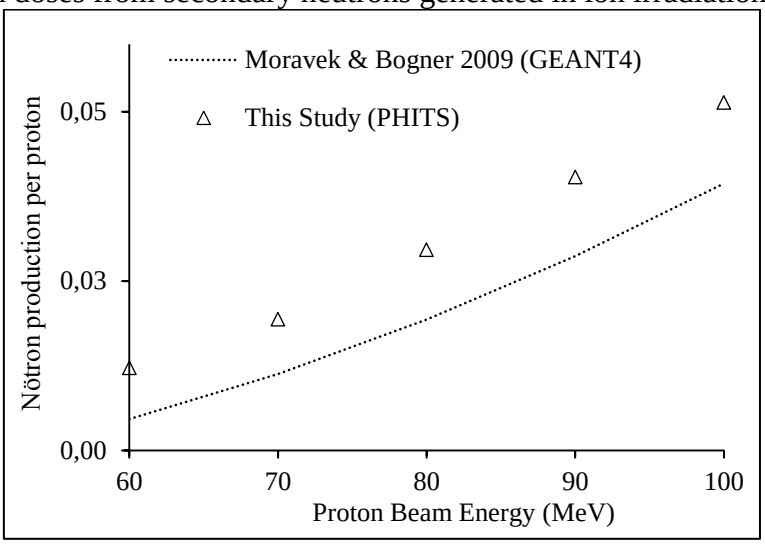

Figure 2. Comparison of secondary neutron generation versus incoming proton energy in a water phantom with the literature

In the simulated head phantom, secondary neutron generation and absorbed dose calculations were made for proton and helium ions in the energy range of 50-100 MeV/u in 10 MeV steps. Figure 3 shows the number of neutrons produced per particle sent in the slab head phantom. It was seen that the agreement of our results with the results of the study with the MCNP MC simulation code was excellent [25]. As the particle energy increases, so does secondary neutron production [25, 32]. It has been reported that as the atomic number of the incident particle increases, the number of SNP in the water phantom increases [23]. While a similar situation is observed in our results, the number of SNP increases when the mass number of the particle sent at the same range of energies increases. When He ion beams were sent, the number of SNP compared to proton beams increased 7-14 times.

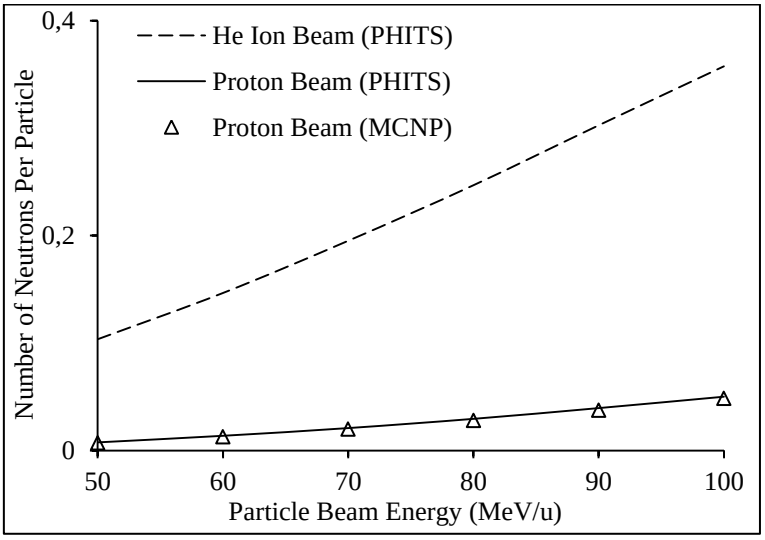

Figure 3. Comparison of the secondary neutron produced in the plate head phantom with the literature [25] and particle type

The dose deposited by neutrons with energies less than 20 MeV produced in the head phantom are shown in Figure 4. The dose for the sent particles with (50-100) MeV/u

energies increased 8.7, 6.7, 6.1, 5.5, 5.1, 4.7 times, respectively, in He ion beams compared to proton beams.

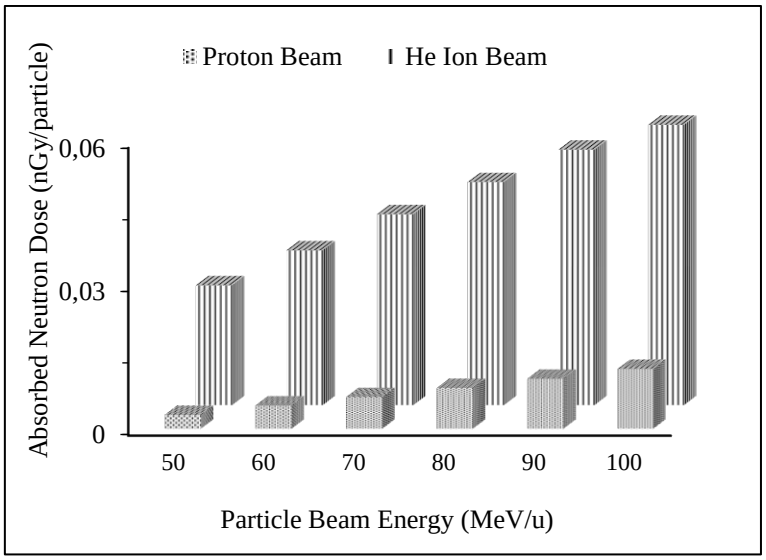

Figure 4. The dose deposited by secondary neutrons in the slab head phantom

Figure 5 shows the total doses deposited by all particles. At all selected energies, the total dose deposited by helium ion beams relative to proton beams increased 4 times. The ratio of the dose deposited by the secondary neutrons in the head phantom to the total deposited dose is shown in Figure 6. When the incoming proton and helium ions are sent to the head phantom, the total absorbed dose in the target and the deposited neutron dose increase linearly as the particle mass number increases. However, the N_D/T_D results were seen to vary between 0.4-0.8 per thousand.

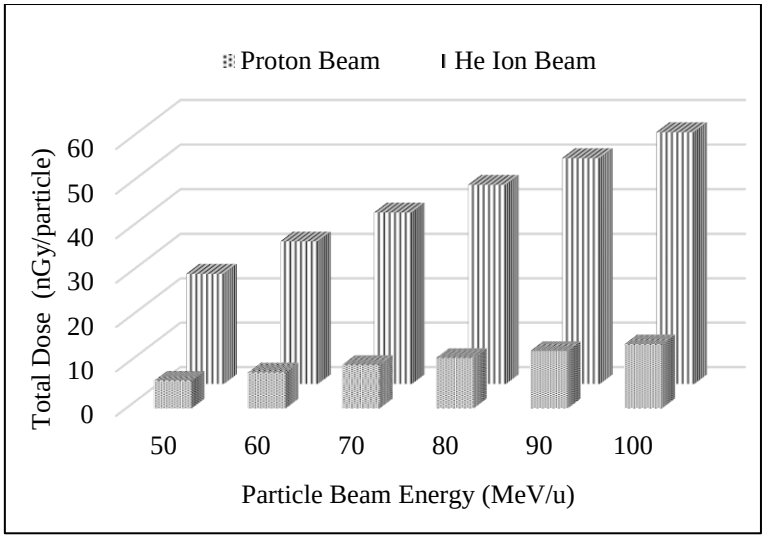

Figure 5. Total deposited dose in the slab head phantom

In the energies of He ion beams, the ratio was found to be constant at around one per thousand. The difference in results can be explained by the variation in neutron generation cross-sections depending on the type and energy of the sent particle and the atomic properties of the target material. In the case of comparing proton and helium ion beams, the N_D/T_D ratio of helium ion beams is higher than that of proton beams. It means that the rate of increase of deposited dose by neutrons is higher than the rate of increase of deposited dose by all particles.

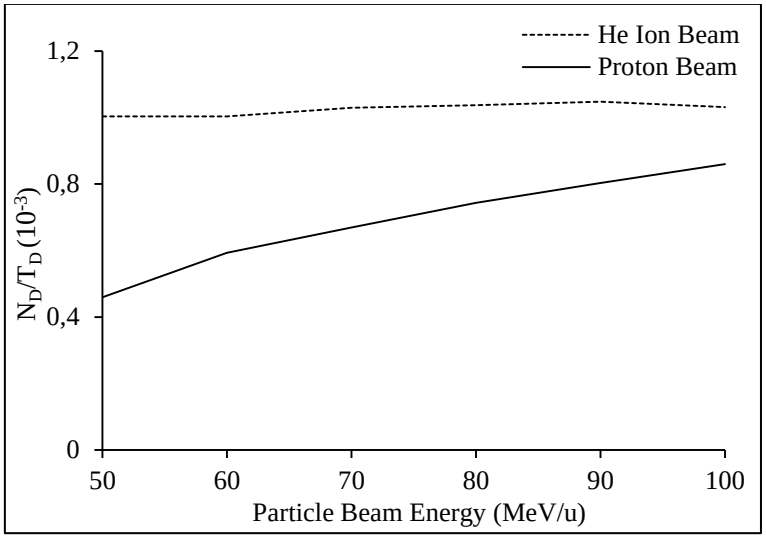

Figure 6. The ratio of dose deposited by secondary neutrons to total deposited dose in the slab head phantom (N_D/T_D)(10^{-3})

4. Conclusion and Comment

The number of neutrons with energies greater than 5 MeV for every 200 MeV/u incoming helium ion into the tissue is one per incident particle, while the number of secondary neutrons is reported to be 0.05, 0.2 and 0.4 per proton with 100, 200 and 300 MeV energies, respectively [35]. In the slab head phantom in our study, while the number of SNP per particle for 200 MeV/u He ion was 0.65, it was found to be 0.048, 0.013 and 0.013 per proton with 100, 200 and 300 MeV energies. The reason the SNP is the same is that the Bragg-peaks of the 200MeV and 300MeV protons do not remain in the phantom. Since they do not release energy to the environment, the result is different from the literature. As for the 100MeV protons, the SNP is in good agreement with the literature. Since Bragg-peaks of helium ions with 200MeV/u energy are also out of the phantom, it has been observed that the number of SNP in the medium is lower than the result in the Ref 35.

In general, neutron doses are much lower than the total deposited dose by the incoming particles. It has been reported that the neutron dose at the Bragg peak depth in the water phantom cannot exceed 0.7% of the total dose for protons with 70 MeV energies [36]. In our study, it was calculated that the secondary neutron doses for protons with 50-100 MeV energies in the entire head phantom varied between 0.4 and 0.8 per thousand of the total dose. The reason for the 10 times difference compared to the literature is that the N_D/T_D ratio is calculated not only in the central axis (beamline) but also in the entire head phantom.

It is known that He ion beams have a better ratio of peak dose to input dose than proton beams [37]. However, it has been reported that the number of neutrons produced by protons with an energy of 202 MeV/u is approximately 25% of the number of neutrons produced by He ions in the cylindrical water phantom [23]. In our study, the number of neutrons produced in the head phantom for protons with an energy of 100 MeV/u is approximately 14% of the number of neutrons produced by He ions with the same energy. The deposited doses by the neutrons produced by the proton beams at selected energies range from 11.5% to 16.4% of the deposited doses by the neutrons produced by the He ion beams. The obtained results are given in Figure 4 and 5 as nGy per particle.

It is known that the high neutron flux produced by ion beams, in which patient tissues cannot be protected, has the potential to cause some detrimental effects, including the induction of new primary cancers [8]. These neutrons will also influence the observed RBE of the particles considered in total dose equivalent estimation and treatment planning. Our MC simulation study is based on the results of SNP by sending pencil beam monoenergetic protons and He ions to the head phantom. The results show that it is feasible to simulate neutron energy spectra at the target or phantom when it is not possible to obtain information about neutrons through clinical studies. Experimental studies for secondary neutron calculations in PT are ongoing all over the world. The development of simulated neutron calculations will be beneficial not only for biological experiments, but also for physics experiments such as the development and calibration of neutron dosimeters [38]. The results we obtained allow us to compare the dose absorbed by the produced secondary neutrons with the desired dose. Therefore, it guides the determination of the particle to be used. The higher mass number of particles reaching the same range, causes more neutron production and releases more neutron dose. It is recommended that secondary neutron production from tissue and its effects be thoroughly investigated during PT. In future studies, equivalent doses absorbed in slab and other phantom types can be investigated through MC simulation codes.

Author Statement

Adem Pehlivanlı: Investigation, Validation, Visualization, Original Draft Writing, Formal Analysis
Mustafa Hicabi Bölükdemir: Investigation, Methodology, Review and Editing, Supervision, Observation, Advice

Acknowledgment

As the authors of this study, we declare that we do not have any support and thank you statement. This study is derived from Adem Pehlivanlı's doctoral thesis.

Conflict of Interest

As the authors of this study, we declare that we do not have any conflict of interest statement.

Ethics Committee Approval and Informed Consent

As the authors of this study, we declare that we do not have any ethics committee approval and/or informed consent statement.

References

[1] V. Giacometti, G. Battistoni, M. De Simoni, Y. Dong, M. Fischettic, E. Gioscio, *et al.*, "Characterisation of the MONDO detector response to neutrons by means of a FLUKA Monte Carlo simulation," *Radiat. Meas.*, 119, 144–149, 2018.

[2] F. Tommasino, E. Scifoni, and M. Durante, "New ions for therapy," *Int. J. Part. Ther.*, 2 (3), 428–438, 2015.

[3] M. Lodge, M. Pijls-Johannesma, L. Stirk, A. J. Munro, D. De Ruysscher, and T. Jefferson, "A systematic literature review of the clinical and cost-effectiveness of hadron therapy in cancer," *Radiother. Oncol.*, 83 (2), 110–122, 2007.

[4] I. Mattei, F Bini, F Collamati, E De Lucia, P M Frallicciardi, E Iarocci, C Mancini-Terracciano, *et al.*, "Secondary radiation measurements for particle therapy applications: Prompt photons produced by 4He, 12C and 16O ion beams in a PMMA target," *Phys. Med. Biol.*, 62 (4), 1438–1455, 2017

[5] D. A. S. C. Rtner *et al.*, "Results of Carbon Ion Radiotherapy in 152 Patients," *Int. J. Radiation Oncology Biol. Phys.*, 58 (2), 631–640, 2004.

[6] J. R. Castro, D. E. Linstadt, J. P. Bahary, P. L. Petti, I. Daftari, J. M. Collier, *et al.*, "Experience in charged particle irradiation of tumors of the skull base: 1977-1992," *Int. J. Radiat. Oncol. Biol. Phys.*, 29 (4), 647–655, 1994.

[7] D. Schulz-Ertner and H. Tsujii, "Particle radiation therapy using proton and heavier ion beams," *J. Clin. Oncol.*, 25 (8), 953–964, 2007.

[8] E. Gioscio, G. Battistoni, A. Bochetti, M. De Simoni, Y. Dong, M. Fischetti, *et al.*, "Development of

a novel neutron tracker for the characterisation of secondary neutrons emitted in Particle Therapy," *Nucl. Instruments Methods Phys. Res. Sect. A Accel. Spectrometers, Detect. Assoc. Equip.*, 958 (162862), 1-4, 2020.
[9] G. Baiocco, S. Barbieri, G. Babini, J. Morini, D. Alloni, W. Friedland, *et al.*, "The origin of neutron biological effectiveness as a function of energy," *Sci. Rep.*, 6 (34033), 1–14, 2016.
[10] T. Kajimoto, K. Tanaka, S. Endo, S. Kamada, H. Tanaka, M. Takada and T. Hamano, "Double differential cross sections of neutron production by 135 and 180 MeV protons on A-150 tissue-equivalent plastic," *Nucl. Instruments Methods Phys. Res. Sect. B Beam Interact. with Mater. Atoms*, 487, 38–44, 2021.
[11] K. Kurosu, I. J. Das, and V. P. Moskvin, "Optimization of GATE and PHITS Monte Carlo code parameters for spot scanning proton beam based on simulation with FLUKA general-purpose code," *Nucl. Instruments Methods Phys. Res. Sect. B Beam Interact. with Mater. Atoms*, 367, 14–25, 2016.
[12] C. M. Lund, G. Famulari, L. Montgomery, and J. Kildea, "A microdosimetric analysis of the interactions of mono-energetic neutrons with human tissue," *Phys. Medica*, 73 (April), 29–42, 2020
[13] U. Titt, B. Bednarz, and H. Paganetti, "Comparison of MCNPX and Geant4 proton energy deposition predictions for clinical use," *Phys. Med. Biol.*, 57 (20), 6381–6393, 2012.
[14] D. J. Brenner, C. D. Elliston, E. J. Hall, and H. Paganetti, "Reduction of the secondary neutron dose in passively scattered proton radiotherapy, using an optimized pre-collimator/collimator," *Phys. Med. Biol.*, 54 (20), 6065–6078, 2009.
[15] R. A. Cecil, B. D. Anderson, A. R. Baldwin, and R. Madey, "Neutron angular and energy distributions from 710-MeV alphas stopping in water, carbon, steel, and lead, and 640-MeV alphas stopping in lead," *Phys. Rev. C*, 21 (6), 2471–2484, 1980.
[16] L. Heilbronn, R. S. Cary, M. Cronqvist, F. Deák, K. Frankel, A. Galonsky, *et al.*, "Neutron yields from 155 MeV/nucleon carbon and helium stopping in aluminum," *Nucl. Sci. Eng.*, 132 (1), 1–15, 1999.
[17] L. Heilbronn, C. J. Zeitlin, Y. Iwata, T. Murakami, H. Iwase, T. Nakamura, *et al.*, "Secondary neutron-production cross sections from heavy-ion interactions between 230 and 600 MeV/nucleon," *Nucl. Sci. Eng.*, 157 (2), 142–158, 2007.
[18] T. Kurosawa *et al.*, "Measurements of secondary neutrons produced from thick targets bombarded by high-energy helium and carbon ions," *Nucl. Sci. Eng.*, 132 (1), 30–57, 1999.
[19] T. Kurosawa, T. Nakamura, N. Nakao, T. Shibata, Y. Uwamino, and A. Fukumura, "Spectral measurements of neutrons, protons, deuterons and tritons produced by 100 MeV/nucleon He bombardment," *Nucl. Instruments Methods Phys. Res. Sect. A Accel. Spectrometers, Detect. Assoc. Equip.*, 430 (2–3), 400–422, 1999.
[20] H. Sato, T. Kurosawa, H. Iwase, T. Nakamura, Y. Uwamino, and N. Nakao, "Measurements of double differential neutron production cross sections by 135 MeV/nucleon He, C, Ne and 95 MeV/nucleon Ar ions," *Phys. Rev. C - Nucl. Phys.*, 64 (034607), 1–12, 2001.
[21] P. Ortego, "Benchmarking of MCNPX with the experimental measurements of high-energy helium ions in HIMAC facility," *Radiat. Prot. Dosimetry*, 116 (1–4), 43–49, 2005.
[22] K. W. Delinder, R. Khan, and J. L. Gräfe, "Neutron activation of gadolinium for ion therapy: a Monte Carlo study of charged particle beams," *Sci. Rep.*, 10 (1), 1–11, 2020.
[23] I. Gudowska and N. Sobolevsky, "Simulation of secondary particle production and absorbed dose to tissue in light ion beams," *Radiat. Prot. Dosimetry*, 116 (1–4), 301–306, 2005.
[24] P. E. Tsai, L. H. Heilbronn, B. L. Lai, Y. Iwata, T. Murakami, and R. J. Sheu, "Thick target neutron yields from 100- and 230-MeV/nucleon helium ions bombarding water, PMMA, and iron," *Nucl. Instruments Methods Phys. Res. Sect. B Beam Interact. with Mater. Atoms*, 449, 62–70, 2019
[25] S. B. Jia, M. H. Hadizadeh, A. A. Mowlavi, and M. E. Loushab, "Evaluation of energy deposition and secondary particle production in proton therapy of brain using a slab head phantom," *Reports Pract. Oncol. Radiother.*, 19 (6), 376–384, 2014.
[26] R. Behrens and O. Hupe, "Influence of the phantom shape (slab, cylinder or alderson) on the performance ofan Hp(3) eye dosemeter," *Radiat. Prot. Dosimetry*, 168 (4), 441–449, 2015
[27] D. R. White, R. V. Griffith and I. J. Wilson, "ICRU Report 46: Photon, electron, proton and neutron interaction data for body tissues." *Journal of the ICRU*, 24 (1), 5-9, 1992
[28] H. M. Kooy *et al.*, "A case study in proton pencil-beam scanning delivery," *Int. J. Radiat. Oncol. Biol. Phys.*, 76 (2), 624–630, 2010.
[29] K. Iida, A. Kohama, and K. Oyamatsu, "Formula for proton-nucleus reaction cross section at intermediate energies and its application," *J. Phys. Soc. Japan*, 76 (4), 1–6, 2007.
[30] T. Sato *et al.*, "Features of particle and heavy ion transport code system (PHITS) version 3.02," *J. Nucl. Sci. Technol.*, 55 (6), 684–690, 2018.
[31] A. Boudard, J. Cugnon, J. C. David, S. Leray, and D. Mancusi, "New potentialities of the Liège intranuclear cascade model for reactions induced by nucleons and light charged particles," *Phys.*

Rev. C - Nucl. Phys., 87 (1), 2013.
[32] Z. Morávek and L. Bogner, "Analysis of the physical interactions of therapeutic proton beams in water with the use of Geant4 Monte Carlo calculations," *Z. Med. Phys.*, 19 (3), 174–181, 2009ç
[33] U. Schneider, S. Agosteo, E. Pedroni, and J. Besserer, "Secondary neutron dose during proton therapy using spot scanning," *Int. J. Radiat. Oncol. Biol. Phys.*, 53 (1), 244–251, 2002ç
[34] A. J. Wroe, I. M. Cornelius, and A. B. Rosenfeld, "The role of nonelastic reactions in absorbed dose distributions from therapeutic proton beams in different medium," *Med. Phys.*, 32 (1), 37–41, 2005.
[35] M. A. Chaudhri, "Neutron production from patients during therapy with bremsstrahlung and hadrons: Are there potential risks with hadrons, especially with carbon ions?," *IFMBE Proc.*, Nuernberg, 2007, pp. 2207–2210.
[36] A. Dawidowska, M. P. Ferszt, and A. Konefał, "The determination of a dose deposited in reference medium due to (p,n) reaction occurring during proton therapy," *Reports Pract. Oncol. Radiother.*, 19, 3–8, 2014.
[37] J. Kempe, I. Gudowska, and A. Brahme, "Depth absorbed dose and LET distributions of therapeutic 1H, 4He, 7Li, and 12C beams," *Med. Phys.*, 34 (1), 183–192, 2007.
[38] S. Yonai and S. Matsumoto, "Monte Carlo study toward the development of a radiation field to simulate secondary neutrons produced in carbon-ion radiotherapy," *Radiat. Phys. Chem.*, 172, 1-9, 2020.